Polar Effects on the Thermal Conductivity of Cubic Boron Nitride under Pressure

Saikat Mukhopadhyay[1] and Derek A. Stewart[1,*]

[1]*Cornell Nanoscale Facility, Cornell University, 250 Duffield Hall, Ithaca, New York 14853, USA*

We report the lattice thermal conductivity (κ) of cubic boron nitride (c-BN) under pressure calculated using density functional theory. Pressure was used to manipulate the c-BN phonon dispersion and study its effect on thermal conductivity. These results were compared to c-BN's mass-equivalent, nonpolar counterpart, diamond, in order to isolate the effect of polar bonds on thermal conductivity. Unlike diamond, the variation of κ at room temperature (κ_{RT}) with applied pressure in c-BN is nonlinear in the low-pressure regime followed by a transition to a linear regime with a distinct change in the slope at $P > 114$ GPa. We find that the change in κ with pressure cannot be described with power law expressions commonly used for Earth mantle materials. The nonlinearity in the low-pressure regime can be related to the nonlinear change in LO-TO gap, group velocities, and specific heat with increasing pressure. In addition, we find that, although optical branch contributions to thermal conductivity are small ($\sim$2% at RT), the rise in κ_{RT} for $P > 114$ GPa is due to (1) the decoupling of the longitudinal acoustic branch from the optical branches and (2) depopulation of the optical branches. These lead to a sharp reduction in acoustic-acoustic-optic (a-a-o) scattering and a discrete change in the acoustic phonon mean free paths. This study illustrates the importance of optical branches and their interactions with acoustic branches in determining the total thermal conductivity of polar materials. This finding is also relevant for current research in geologic minerals under pressure and the design of thermoelectrics.

The last decade has seen a renaissance in the study and understanding of thermal conductivity (κ) in materials and nanostructures, driven largely by new *ab initio* Boltzmann transport approaches [1–6], large-scale molecular dynamics simulations [7–10], and novel κ measurement techniques [11–13]. These approaches offer an unprecedented window into the secret life of phonons, providing, for the first time, accurate estimates for (1) normal and umklapp scattering rates in crystals [2,14], (2) thermal conductivity accumulation function [11,15,16], and (3) the often underestimated role of optical phonons [17,18]. These insights have led to the prediction of new high κ materials (e.g., BAs [19]), techniques for improving thermoelectrics [20,21], and κ estimates for minerals deep in the Earth [6,22].

While the thermal conductivities of numerous materials have been calculated from first principles recently, a fundamental question of how thermal transport in polar materials differs from their nonpolar counterparts is still unresolved. The answer to this question also has practical implications for fields ranging from heat flow in Earth mantle materials to thermoelectrics design. It is well known that long-range Coulomb interactions between ions in a polar system result in a nonanalytic term in the dynamical matrix that depends on the Born effective charge Z^* and dielectric constant ε_∞. This term leads to Lydanne-Sachs-Teller splitting of the longitudinal and transverse optical modes at the Γ point [23]. While it is clear that long-range Coulomb interactions significantly change the phonon dispersion of polar materials, evidence for a direct effect on κ has been inconclusive. Optical phonons typically have small group velocities and do not contribute directly to thermal transport [17,18]. Further, LO-TO splitting usually does not lead to major changes in group velocity near the Γ point; therefore, its effect on κ is often neglected. However, optical phonons do play a key role in scattering acoustic phonons [2]. In this case, LO-TO splitting may appreciably affect acoustic thermal transport. Coulomb interactions push the LO branch to higher frequencies and could significantly alter the phase space for phonon-phonon scattering and the resulting thermal conductivity. As a counter-point, one could argue that changes in phase space would be localized at Γ and this would lead to a small change in κ. For low κ systems, it is reasonable to assume that this effect would be small compared to other scattering mechanisms. Therefore, the best candidate to isolate polar effects would be a high κ polar system with a small number of phonon branches and a correspondingly small phase space for phonon-phonon scattering.

Cubic boron nitride (c-BN) has a two-atom zinc blende crystal structure, a sizable LO-TO splitting ($\sim$227 cm^{-1} at Γ), and a wide LO-TO gap for most of the Brillouin zone. Previously examined polar systems do not present ideal systems for isolating LO-TO effects. GaN has fairly large LO-TO splitting [24], but the significant phonon band gap between GaN optical and acoustic branches plays a dominant role in determining κ. By contrast, c-BN optical branches are situated at the top of the acoustic branches with TO phonon branches overlapping the LA branch at

multiple Brillouin zone points. On the other extreme, BAs [19] was recently shown to have a κ potentially higher than diamond, but its LO-TO splitting is too small (~ 3 cm^{-1}) to be significant. In this letter, we examine the variation of κ in c-BN over a wide pressure range, which enables us to manipulate LO-TO splitting, the position of acoustic and optical branches, and the anharmonic interatomic force constants. This provides a physical knob to adjust the polar nature of c-BN and understand its impact on κ. A further benefit of c-BN is that diamond provides a suitable and well-studied nonpolar analogue.

The lattice thermal conductivity was calculated using a first-principles approach *without any adjustable parameters*, where harmonic and anharmonic interatomic force constants (IFCs) are determined using density functional perturbation theory (DFPT). Our calculations are done within the local density approximation (LDA) and Bachlet-Hamann-Schlüter [25] pseudopotentials were used for all atoms. A $8 \times 8 \times 8$ Monkhorst-Pack k-point grid, $4 \times 4 \times 4$ q-mesh and a 120 Ry cutoff energy were used to calculate the harmonic IFCs. Third order anharmonic IFCs were calculated at 0 K and include interactions out to seventh nearest neighbors [2,26]. For heat flow along z direction, κ is [2]:

$$\kappa_{zz} = \frac{1}{V}\sum_{\lambda} C_{\lambda} v_z^2 \tau_{\lambda z}, \qquad (1)$$

where V is crystal volume, C_{λ} is mode specific heat, and v_z is group velocity along z. We use the shorthand $\lambda = (j, \vec{q})$ where j and $\vec{q}$ are phonon branch and wave vector, respectively. Specific heat and group velocity are calculated using harmonic IFCs, while third order anharmonic IFCs are required to calculate scattering times ($\tau_{\lambda z}$). Scattering times are obtained by iteratively solving the linearized Boltzmann transport equation [1,2,27] (see Supplemental Material [28] for details):

$$\frac{\partial n_{\lambda}}{\partial t}\bigg|_{\text{collision}} = \vec{v_{\lambda}}\cdot\nabla T \frac{\partial n_{\lambda}^0}{\partial T}, \qquad (2)$$

where T is temperature and the perturbed phonon distribution is given by $n_{\lambda} = n_{\lambda}^0 + n_{\lambda}^{ne}$ where n_{λ}^0 is the equilibrium Bose-Einstein phonon distribution and the nonequilibrium portion, n_{λ}^{ne}, is proportional to ∇T. The collision term is solved explicitly and considers phonon-phonon scattering based on Fermi's Golden rule. We consider all scattering processes in the phase space (determined by the phonon dispersion and the q-point sampling grid used) that satisfy conservation of energy, $\omega_j(\vec{q}) \pm \omega_{j'}(\vec{q}\,') = \omega_{j''}(\vec{q}\,'')$, and crystal momentum $\vec{q} \pm \vec{q}\,' = \vec{q}\,'' + \vec{K}$, where $\vec{K} = 0$ ($\vec{K} \neq 0$) for normal (umklapp) processes. To isolate effects due to the polar nature of c-BN, we consider an isotopically pure system.

Before we investigate pressure effects on c-BN thermal conductivity, a brief review is necessary to verify our approach. For no applied pressure, our calculated room temperature κ (κ_{RT}) was 2113 W/m-K. Previous theoretical estimates for c-BN κ_{RT} vary widely with predictions

ranging from 850 to 3000 W/m-K [29–31]. This wide spread can be traced to adjustable parameters used to fit experimental data of diamond [31] or to treat N- and U-scattering processes [29,30]. Since experimental estimates of c-BN κ_{RT} (1300 W/m-K) are limited to samples with scatterings from boundaries and impurities [32], the use of empirical approaches with fitted parameters is questionable. Recently, Lindsay *et al.* [19] estimated a similar value (2145 W/m-K) for κ_{RT} from first-principles calculations based on a real space approach considering interactions out to third nearest neighbor. The small κ_{RT} difference (1.5%) between these two approaches could be due to our inclusion of longer range interactions. The difference in κ calculated using DFPT and the real space approach is similar to that found ($< 3\%$) for other polar materials (GaAs and GaP) [33]. The calculated c-BN κ_{RT} was lower than the reported value for diamond (> 3000 W/m-K) using a similar approach [2]. This is qualitatively consistent with experimental measurements [32].

Figure 1(a) shows the calculated κ of isotopically pure c-BN as a function of temperature and pressure. Under applied pressure, c-BN κ increases as was found with diamond [27]; however, the variation of κ with pressure is not linear (white lines along the P axes) for any given temperature [Fig. 1(a)]. The nonlinearity in κ with pressure is more profound in the low temperature regime ($T = 200$–400 K) compared to higher temperatures, $T > 400$ K. To investigate the pressure effect on κ explicitly, the variation of κ_{RT} with pressure at $T = 300$ K is shown in Fig. 1(b). The variation of κ_{RT} in c-BN with pressure can be divided into two different regions. In region I ($P = 0$–114 GPa), κ_{RT} increases nonlinearly with pressure and in region II ($P > 114$ GPa), κ_{RT} increases linearly with pressure with a sharp increase in slope [Fig. 1(b)]. This is in stark contrast to diamond's behavior under pressure [27] where κ increases linearly over a wide pressure range (80–400 GPa) with a slight parabolic section at lower pressures.

The applied pressure was simulated by changing the lattice constant similar to previous work on diamond [27]. The calculated c-BN equation of state is in excellent agreement with experiment [35] (see Fig. S1 in Supplemental Material [28]). The pressure variation with lattice parameter is identical to diamond [27] (see Fig. S1 in Supplemental Material [28]) in the low pressure regime and deviates slightly at higher pressure. This indicates that the polar bonds in c-BN do not affect the equation of state, but do affect κ.

The nonlinearity in Fig. 1(b) for $P < 114$ GPa may be due to the variation of the group velocities (see Fig. S2(a) in Supplemental Material [28]) and specific heat (see Fig. S2(b) in Supplemental Material [28]), which also vary nonlinearly with increasing pressure. However, the $P - \kappa_{\text{RT}}$ relationship cannot be explained based on these alone. To support this argument, we fitted our $P - \kappa_{\text{RT}}$ data, adapting the expression proposed by Hofmeister [34]:
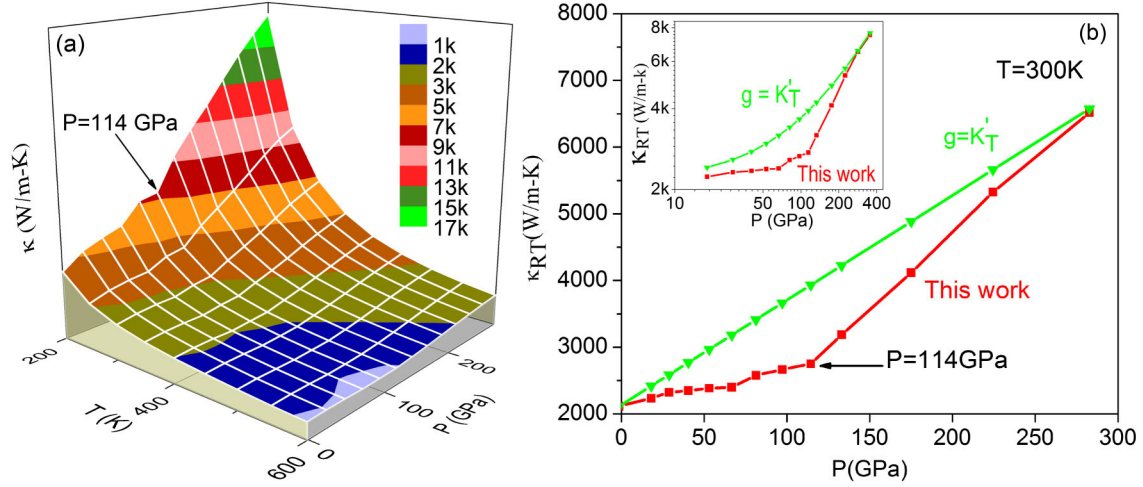
FIG. 1 (color online).   (a) Calculated κ of isotopically pure c-BN versus temperature and pressure. White lines denote temperature (parallel to P axes) and pressure (parallel to T axes) grids. (b) Variation of κ_{RT} of c-BN with pressure (red line with squares). Green line with triangles shows analytical expression [Eq. (3)] from Hofmeister [34] with $g = 3.01$. The log-log inset plot shows the numerical (red) and analytical (green) $P - \kappa_{RT}$ relation for a wider pressure range.

$$\kappa = \kappa_0 \left(\frac{\rho}{\rho_0}\right)^g \left(\frac{T}{T_0}\right), \qquad (3)$$

where $g = (\partial K_T / \partial P)_T = 3.01$ (for c-BN) and K_T is the bulk modulus. ρ and ρ_0 are mass densities at applied pressure and with no applied pressure, respectively. This model assumes the change in group velocity can be approximated by the change in bulk sound velocity [34]. For $T = 300$ K, $T/T_o = 1$, and $\kappa_0 = 2113$ W/m-K, the resulting κ_{RT} using Eq. (3) is shown in Fig. 1(b). It is clear that Eq. (3) does not agree with the calculated $P - \kappa_{RT}$ characteristics of c-BN in the low pressure regime; however, they do concur at much higher pressures, $P > 220$ GPa (Fig. 1(b) inset).

To understand how pressure affects c-BN κ, we examined phonon dispersions at various pressures. Calculated phonon dispersions at $P = 0, 114, 174,$ and 283 GPa are shown in Figs. 2(a)–2(d) and phonon dispersions at additional pressures are listed in Supplemental Material (Fig. S3) [28]. Since the complete c-BN phonon dispersion has not been measured, we compared our calculated $P = 0$ GPa phonon dispersion with available second order Raman-spectra [36] for LO and TO branches and found good agreement (Table 1 of Supplemental Material [28]). The calculated group velocities: 15.11 (15.41 [37]) and 11.22 (11.8 [37]) km/s also agree well with measured values. In the equilibrium geometry, a LO-TO gap occurs at Γ (227 cm^{-1}) [Fig. 2(a)] as well as at X and L high-symmetry points. The LA-branch disperses into the optical branches at X with a significant LA-TO interaction. With applied pressure, the low-frequency TA branches remained unaltered apart from a slight shift to higher frequencies similar to diamond [27]. As pressure increases, the LA branch maximum and the optical branches gradually move up in frequency and the LO-TO gap at Γ reduces non-linearly (Fig. S4 [28]). Under pressure, the LO branch

gradually merges with the TO branches, closing the LO-TO gap at L and at X for $P = 174$ and $P = 283$ GPa, respectively [Figs. 2(c), 2(d)]. This reduces the available phase space for phonon-phonon scattering because phonons with the same energy cannot simultaneously satisfy
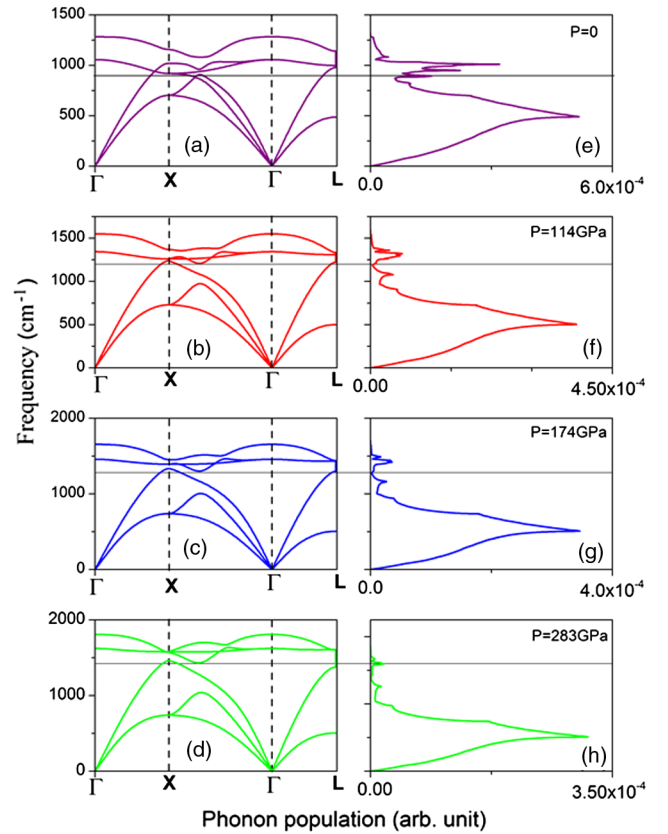

FIG. 2 (color online).   Phonon dispersions of c-BN for (a) $P = 0$, (b) 114 GPa, (c) 174 GPa, and (d) 283 GPa. Room temperature phonon population are shown for (e) $P = 0$, (f) 114, (g) 174, and (h) 283 GPa. Horizontal lines note the lowest optical frequency.

conservation of momentum and energy [38]. Due to the upward movement of the optical branches, the LA-branch starts decoupling from the optical branches with increasing pressure and becomes completely decoupled at $P = 114$ GPa. This acts to reduce a-a-o scattering. These factors culminate in a discrete increase in κ_{RT} at $P > 114$ GPa. These dramatic changes in phonon dispersion due to applied pressure are not common in polar materials. The GaN LO-TO splitting increases slightly, but AlN LO-TO splitting is unaffected by pressure [39]. III–V materials have similar dielectric constants. Therefore, differences in the pressure dependence of LO-TO splitting can be attributed to differences in bond ionicity. The bond ionicity of AlN and GaN (Born effective charge ~ 2.5 [40]) is greater than BN (Born effective charge ~ 1.9, this Letter). Since the charge is localized on the ions, the charge distribution in AlN and GaN does not change significantly [40] with applied pressure. Due to its lower ionicity, external pressure has a more significant effect on the charge distribution in c-BN. This leads to the higher pressure dependency of LO-TO splitting in c-BN compared to AlN and GaN.

A direct correlation between differences in the above mentioned scattering processes and optical phonon populations can be established. Room temperature phonon population, $n(\omega)$ for various pressures were calculated by combining phonon density of states, $D(\omega)$, and Bose-Einstein distribution function at $T = 300$ K as $n(\omega) = D(\omega)/(e^{\hbar\omega/k_B T} - 1)$. The phonon populations for different pressures are shown in Figs. 2(e)–2(h). The horizontal line denotes the lowest optical frequency in each case. At $P = 0$ GPa, both acoustic and optical branches are populated and a-a-a and a-a-o scattering processes can contribute to c-BN κ_{RT}. With increasing pressure, the optical branches begin to depopulate and, at $P = 114$ GPa, a considerable decrease in phonon population occurs [Fig. 2(f)], resulting in a reduction in a-a-o scattering processes. It is interesting to note that at $P = 114$ GPa, κ_{RT} starts to increase linearly. From $P = 174$–283 GPa, the optical branches are almost completely depopulated, freezing out most a-a-o and o-o-a scattering processes. Scattering processes where two acoustic phonons combine to create an optical mode ($a + a \rightarrow o$) could still occur, but the number of ($a + o \rightarrow a$) or ($o \rightarrow a + a$) scattering processes is greatly reduced. This becomes readily apparent if we monitor the number of umklapp and normal scattering processes at each pressure that satisfy momentum and energy conservation for the dense q-grid used. In Fig. 3, we find that the ratio of the number of umklapp processes to the total (umklapp + normal) scattering processes saturates at $P > 174$ GPa. Therefore, for $P > 174$ GPa, since there is very little LA-TO interaction and the optical braches are depopulated, the thermal resistance of the system saturates. Since the anharmonic contribution to κ_{RT} remains constant, any change in κ_{RT} for $P > 174$ GPa is dominated by
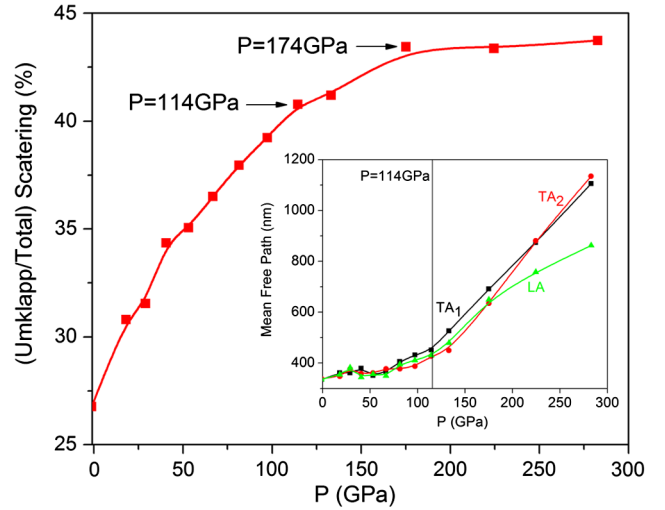

FIG. 3 (color online). Ratio of the number of umklapp to total (umklapp + normal) scattering processes versus pressure. The inset shows RT acoustic phonon mean free paths (MFPs) versus pressure.

changes in harmonic properties such as group velocities and specific heat. Interestingly, in this region, the calculated κ_{RT} approaches the Eq. (3) value.

We also examined how the acoustic phonon mean free paths (MFPs) changed with pressure [Fig. 3 (inset)]. Interestingly, the acoustic branch MFPs remain unaltered until $P = 114$ GPa, where they start increasing sharply. This supports the conclusion that at $P > 114$ GPa the a-a-o and o-o-a scatterings are frozen out, leading to a sharp increase in κ_{RT} [Fig. 1(b)]. κ_{RT} in diamond under pressure increases mainly due to phonon modes shifting to higher frequencies, resulting in weaker phonon-phonon scattering [27]. We find c-BN optical phonons are much more sensitive to external pressure. κ_{RT} with pressure is not only affected by the higher frequency optical modes but also by differing phonon distributions with pressure in the optical branches.

In summary, we used pressure to manipulate the c-BN phonon dispersion and we studied its impact on thermal conductivity by using a linear phonon Boltzmann transport equation that builds on *ab initio* force constants. In sharp contrast to the linear increase observed in diamond, we find the variation of κ_{RT} of c-BN exhibits two different pressure regimes: a nonlinear regime up to $P = 114$ GPa and a linear region for $P > 114$ GPa. With increasing pressure, the LA branch completely decouples from the optical branches and at RT, the optical branches are almost completely depopulated, significantly reducing a-a-o scattering. This leads to saturated thermal resistance due to phonon-phonon scattering and results in a sharp rise in the acoustic phonon mean free paths. As a result, at $P > 114$ GPa, κ_{RT} increases linearly, dictated by group velocities and related harmonic properties when a-a-o scatterings are frozen out and phonon-phonon scattering is dominated by a-a-a scattering. Finally, by manipulating the LO-TO splitting via applied pressure, we showed wide variation of κ in polar materials.

Given that c-BN serves as a pressure gauge in diamond anvil experiments, verification of our predictions should be possible. This study provides new physical insights into the effect of LO-TO splitting on a-a-o scattering processes and offers direct evidence for their role in determining κ in polar materials. This could have important implications for the thermal conductivity of Earth mantle minerals. Hofmeister [34] noted that comparing measured mineral thermal conductivity with analytical models required fitting parameters due to the omission of the pressure dependence of phonon lifetimes. Our first principle study calculates κ directly without adjustable parameters. In addition, the origin of low κ in PbTe was recently traced to coupling between LA and TO branches [41,42]. The LO-TO gap and the localization of TO mode in PbTe are sensitive to small density changes [43]. This suggests that a nonlinear pressure regime for κ may also exist in PbTe thermoelectrics, given that the overlap of optical and acoustic branches may be tuned via external pressure.

---

*derek.stewart@cornell.edu

[1] D. A. Broido, M. Malorny, G. Birner, N. Mingo, and D. A. Stewart, Appl. Phys. Lett. **91**, 231922 (2007).
[2] A. Ward, D. A. Broido, D. A. Stewart, and G. Deinzer, Phys. Rev. B **80**, 125203 (2009).
[3] M. Omini and A. Sparavigna, Phys. Rev. B **53**, 9064 (1996).
[4] J. Garg, N. Bonini, B. Kozinsky, and N. Marzari, Phys. Rev. Lett. **106**, 045901 (2011).
[5] K. Esfarjani, G. Chen, and H. T. Stokes, Phys. Rev. B **84**, 085204 (2011).
[6] X. L. Tang and J. J. Dong, Proc. Natl. Acad. Sci. U.S.A. **107**, 4539 (2010).
[7] Y. P. He, D. Donadio, and G. Galli, Nano Lett. **11**, 3608 (2011).
[8] S. G. Volz and G. Chen, Phys. Rev. B **61**, 2651 (2000).
[9] P. K. Schelling, S. R. Phillpot, and P. Keblinski, Phys. Rev. B **65**, 144306 (2002).
[10] N. de Koker, Phys. Rev. Lett. **103**, 125902 (2009).
[11] A. J. Minnich, J. A. Johnson, A. J. Schmidt, K. Esfarjani, M. S. Dresselhaus, K. A. Nelson, and G. Chen, Phys. Rev. Lett. **107**, 095901 (2011).
[12] K. T. Regner, D. P. Sellan, Z. H. Su, C. H. Amon, A. J. H. McGaughey, and J. A. Malen, Nat. Commun. **4**, 1640 (2013).
[13] M. E. Siemens, Q. Li, R. G. Yang, K. A. Nelson, E. H. Anderson, M. M. Murnane, and H. C. Kapteyn, Nat. Mater. **9**, 26 (2010).
[14] A. Ward and D. A. Broido, Phys. Rev. B **81**, 085205 (2010).
[15] Y. K. Koh and D. G. Cahill, Phys. Rev. B **76**, 075207 (2007).
[16] F. Yang and C. Dames, Phys. Rev. B **87**, 035437 (2013).
[17] M. Asen-Palmer, K. Bartkowski, E. Gmelin, M. Cardona, A. P. Zhernov, A. V. Inyushkin, A. Taldenkov, V. I. Ozhogin, K. M. Itoh, and E. E. Haller, Phys. Rev. B **56**, 9431 (1997).
[18] G. P. Srivastava, J. Phys. Chem. Solids **41**, 357 (1980).
[19] L. Lindsay, D. A. Broido, and T. L. Reinecke, Phys. Rev. Lett. **111**, 02590 (2013).
[20] W. Li, L. Lindsay, D. A. Broido, D. A. Stewart, and N. Mingo, Phys. Rev. B **86**, 174307 (2012).
[21] J. Shiomi, K. Esfarjani, and G. Chen, Phys. Rev. B **84**, 104302 (2011).
[22] N. de Koker, Earth Planet. Sci. Lett. **292**, 392 (2010).
[23] R. H. Lyddane, R. G. Sachs, and E. Teller, Phys. Rev. **59**, 673 (1941).
[24] V. Yu. Davydov, Y. E. Kitaev, I. N. Goncharuk, A. N. Smirnov, J. Graul, O. Semchinova, D. Uffmann, M. B. Smirnov, A. P. Mirgorodsky, and R. A. Evarestov, Phys. Rev. B **58**, 12899 (1998).
[25] G. B. Bachelet, D. R. Hamann, and M. Schluter, Phys. Rev. B **26**, 4199 (1982).
[26] G. Deinzer, G. Birner, and D. Strauch, Phys. Rev. B **67**, 144304 (2003).
[27] D. A. Broido, L. Lindsay, and A. Ward, Phys. Rev. B **86**, 115203 (2012).
[28] See Supplemental Material at http://link.aps.org/supplemental/10.1103/PhysRevLett.113.025901 for further information on the first principle Boltzmann transport approach. Supplemental Material also includes equation of state for c-BN, variation of group velocity and specific heat with pressure, phonon dispersion plots at additional pressures, and LO and TO Γ-point frequencies as a function of pressure.
[29] S. Barman, Europhys. Lett. **96**, 16004 (2011).
[30] D. T. Morelli, and G. A. Slack, *High Lattice Thermal Conductivity Solids* (Springer, New York, 2006), p. 37.
[31] N. V. Novikov, A. P. Podoba, V. M. Perevertailo, S. V. Shmegera, and A. Witek, Diam. Relat. Mater. **9**, 629 (2000).
[32] G. A. Slack, J. Phys. Chem. Solids **34**, 321 (1973).
[33] L. Lindsay, D. A. Broido, and T. L. Reinecke, Phys. Rev. Lett. **109**, 095901 (2012).
[34] A. M. Hofmeister, Proc. Natl. Acad. Sci. U.S.A. **104**, 9192 (2007).
[35] F. Datchi, A. Dewaele, Y. Le Godec, and P. Loubeyre, Phys. Rev. B **75**, 214104 (2007).
[36] S. Reich, A. C. Ferrari, R. Arenal, A. Loiseau, I. Bello, and J. Robertson, Phys. Rev. B **71**, 205201 (2005).
[37] S. F. Wang, Y. F. Hsu, J. C. Pu, J. C. Sung, and L. G. Hwa, Mater. Chem. Phys. **85**, 432 (2004).
[38] J. R. Olson, R. O. Pohl, J. W. Vandersande, A. Zoltan, T. R. Anthony, and W. F. Banholzer, Phys. Rev. B **47**, 14850 (1993).
[39] A. R. Goñi, H. Siegle, K. Syassen, C. Thomsen, and J. M. Wagner, Phys. Rev. B **64**, 035205 (2001).
[40] S. Q. Wang and H. Q. Ye, J. Phys. Condens. Matter **17**, 4475 (2005).
[41] O. Delaire *et al.*, Nat. Mater. **10**, 614 (2011).
[42] T. Shiga, J. Shiomi, J. Ma, O. Delaire, T. Radzynski, A. Lusakowski, K. Esfarjani, and G. Chen, Phys. Rev. B **85**, 155203 (2012).
[43] Y. Zhang, X. Z. Ke, C. F. Chen, J. Yang, and P. R. C. Kent, Phys. Rev. B **80**, 024304 (2009).